Schweizerische Eidgenossenschaft
Confédération suisse
Confederazione Svizzera
Confederaziun svizra

Département fédéral de l'environnement,
des transports, de l'énergie et de la communication DETEC

Office fédéral de l'énergie OFEN
Section Cleantech

Rapport final du 6 Février 2018

PMU-based Real-time State Estimation of the 125 kV Sub-transmission Network of Lausanne

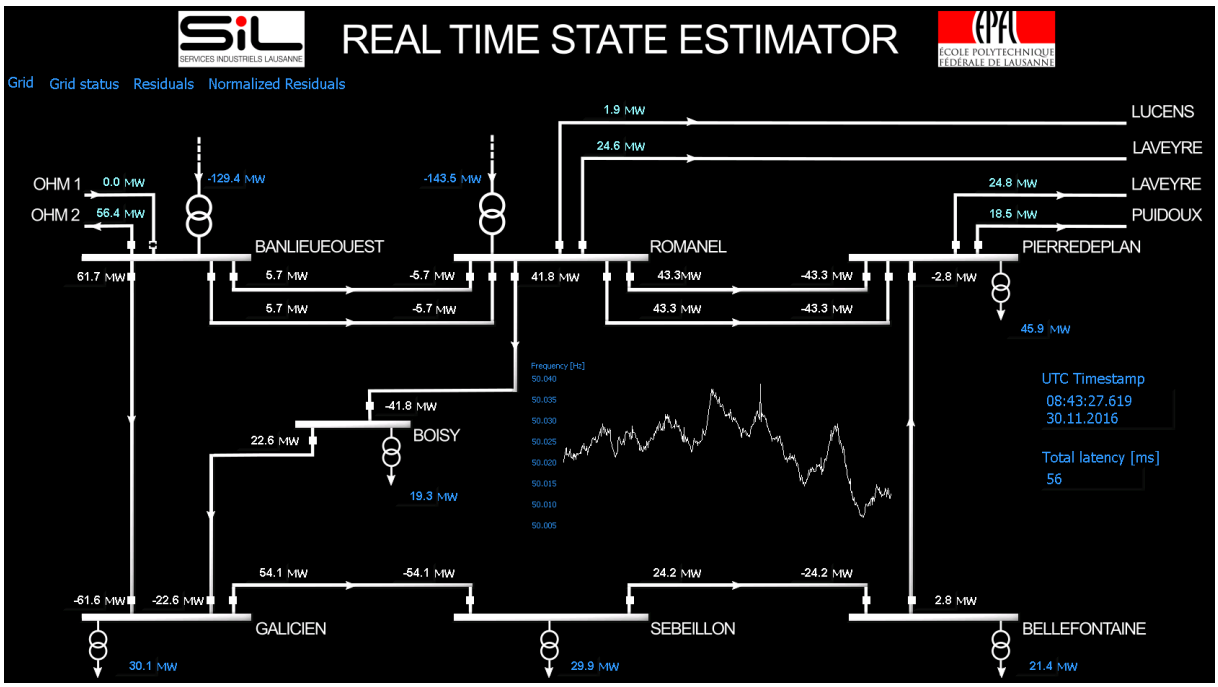

Date : 6 Février 2018

Lieu : Lausanne

Prestataire de subventions :
Confédération suisse, représentée par
L'Office fédéral de l'énergie OFEN
Programme pilote, de démonstration et Programme-phare
CH-3003 Berne
www.ofen.admin.ch

Bénéficiaires de la subvention :
Service de l'électricité de Ville de Lausanne (SEL)
Place Chauderon 27
CH-1003 Lausanne
www.lausanne.ch/sil

Ecole Polytechnique Fédérale de Lausanne
Distributed Electrical System Laboratory (DESL)
EPFL STI IEL DESL Station 11
CH-1015 Lausanne
desl-pwrs.epfl.ch/

Ecole Polytechnique Fédérale de Lausanne
Power Systems Grpoup (PWRS)
EPFL STI GR SCI IEL Station 11
CH-1015 Lausanne
desl-pwrs.epfl.ch/

Auteurs :
Lorenzo Zanni, DESL, lorenzo.zanni@epfl.ch
Yves Dijamatovic, SEL, yves.dijamatovic@lausanne.ch
Mario Paolone, DESL, mario.paolone@epfl.ch
Rachid Cherkaoui, PWRS, rachid.cherkaoui@epfl.ch

Direction du programme de l'OFEN : Yasmine Calisesi, yasmine.calisesi@bfe.admin.ch
Suivi du projet pour l'OFEN : Michael Moser, michael.moser@bfe.admin.ch
Numéro du contrat de l'OFEN : SI/501080-01

Les auteurs sont seuls responsables du contenu et des conclusions de ce rapport.

Office fédéral de l'énergie OFEN
Mühlestrasse 4, 3063 Ittigen, Adresse postale : 3003 Berne
Tél. +41 58 462 56 11 · fax +41 58 463 25 00 · contact@bfe.admin.ch · www.ofen.admin.ch

Abstract

The main goal of this project is to validate in a real electrical power-grid the performance of a distributed monitoring system based on Phasor Measurement Units (PMUs). This system is composed of PMUs located in different nodes of the grid, which send synchrophasor measurements to a data collection point called Phasor Data Concentrator (PDC) through a telecommunication network; in the computer hosting the PDC, the measurements are processed by means of power-system State Estimation (SE) that computes the most likely state of the grid. Thanks to the use of PMU measurements, SE can be computed several times per second, so that it can follow very quick variations of the grid state; such kind of SE is called Real-Time State Estimation (RTSE).

First, in this report we present the design principles of a PDC that implements both the absolute and relative time data pushing logics together with a third one that aims at minimizing the latency introduced by the PDC without increasing the data incompleteness, as suggested in the IEEE Guide C37.244-2013. By referring to the PMU installation in the sub-transmission network of the city of Lausanne, the aforementioned PDC logics are compared in terms of reliability, determinism and reduction of the overall latency. The telecommunication network is based on optical-fiber links that transmit synchrophasor data that are measured by 15 PMUs. The experimental results show that the push-when-complete logic is characterized by the lowest latency, whereas the absolute time logic better mitigates the synchrophasor data latency variations.

Second, we present the implementation and results of PMU-based RTSE for a portion of the 125-kV sub-transmission network of the city of Lausanne. We analyze the accuracy and computational performance of a RTSE that implements the widely used linear weighted least-squares algorithm.

Résumé

L'objectif principal de ce projet est de valider pour un réseau électrique réel les performances d'un système de surveillance distribué s'appuyant sur des unités de mesure de phaseurs (PMU). Ce système est composé de PMU situés dans différents nœuds du réseau. Ils envoient des mesures de synchrophaseur (phaseurs de tensions/courant) à un point de collecte de données appelé Phasor Data Concentrator (PDC) à travers un réseau de télécommunication. Dans l'ordinateur hébergeant le PDC, les mesures sont traitées au moyen de l'estimation d'état (SE) du réseau qui calcule l'état le plus probable de ce réseau. Grâce à l'utilisation de mesures PMU, l'estimation d'état peut être calculé plusieurs fois par seconde, de sorte qu'il peut suivre des variations très rapides de l'état du réseau. Ce type de SE est appelé estimation en temps réel (RTSE).

Dans un premier temps, nous présentons les principes de conception d'un PDC qui implémente à la fois les logiques de données absolues et relatives, ainsi qu'une troisième logique qui minimise la latence introduite par le PDC sans augmenter l'incomplétude des données, comme le suggère l'IEEE Guide C37.244-2013. En se référant à l'installation PMU dans le réseau de transport de la ville de Lausanne, les logiques PDC susmentionnées sont comparées en termes de fiabilité, de déterminisme et de réduction de la latence globale. Le réseau de télécommunication est basé sur des liaisons fibre optique qui transmettent des données de synchrophaseur mesurés par 15 UGP. Les résultats expérimentaux montrent que la logique « push-when-complete » est caractérisée par la latence la plus faible, alors que la logique temporelle absolue atténue mieux les variations de la latence des données du synchrophaseur.

Deuxièmement, nous présentons la mise en œuvre et les résultats de RTSE basé sur le PMU pour une partie du réseau de transport 125 kV de la ville de Lausanne. Nous analysons la précision et la performance computationnelle d'un RTSE implémentant l'algorithme couramment utilisé des moindres carrés.

Zusammenfassung

Das Hauptziel dieses Projektes besteht darin, ein verteiltes Überwachungssystem (englisch: Distributed Monitoring System) für Verteilnetze in einem real existierenden Verteilnetz zu erproben. Das besagte Überwachungssystem verwendet zeitsynchronisierte Zeigermessgeräte (englisch: Phasor Measurement Units / PMUs), die in verschiedenen Knotenunkten des Netzes platziert werden. Diese PMUs senden die gemessenen Phasoren über ein Telekommunikationsnetz an einen Datensammelpunkt (englisch: Phasor Data Concentrator / PDC). Dort werden die Messwerte nicht nur gesammelt, sondern auch zum Zweck der Netzzustandserkennung (englisch: Power System State Estimation / SE) weiterverwendet. Genauer gesagt wird der Netzzustand mithilfe einer Maximalwahrscheinlichkeitsmethode ermittelt. Die Verwendung von PMUs gestattet es, den SE-Prozess mehrere Male pro Sekunde durchzuführen. Dies ermöglicht es wiederum, selbst rasche Veränderungen des Netzzustandes nachzuvollziehen. In diesem Zusammenhang spricht man daher von „Netzzustandserkennung in Echtzeit“ (englisch: Real-Time State Estimation / RTSE).

Der vorliegende Bericht gliedert sich inhaltlich zwei Teile:

Zum Ersten stellen wir ein Konstruktionsprinzip für einen PDC vor, der Messdaten auf dreierlei Weise verarbeiten kann: mit Hilfe absoluter Zeitmarken, relativer Zeitmarken, oder unter Minimierung der durch den PDC verursachten Latenz (englisch: „push-when-complete“). Die letztgenannte Methode ist in Einklang mit der IEEE Richtlinie C37.244-2013 so konzipiert, dass durch sie keine zusätzlichen Datenverluste entstehen. Die drei Verarbeitungsmechanismen vergleichen wir anhand der PMU-Installation im Stromnetz der Stadt Lausanne in puncto Zuverlässigkeit, Determinismus, und kumulierter Latenz. Die Installation besteht aus 15 PMUs, welche an ein Glasfasernetz-Telekommunikationsnetz angeschlossen sind. Die Versuchsergebnisse zeigen, dass der „push-when-complete“ Ansatz die tiefste kumulierte Latenz erreicht, wohingegen die anderen Methoden besser mit Verzögerungen der Messwerte umzugehen vermögen.

Zum Zweiten präsentieren wir eine Umsetzung eines PMU-basierten RTSE in die Praxis, durchgeführt in einem Teil des 125kV-Unterverteilnetz der Stadt Lausanne, sowie die daraus gewonnenen Resultate. In diesem Zusammenhang analysieren wir sowohl die Genauigkeit als auch die Leistungsfähigkeit des verwendeten RTSE, der auf der Methode der kleinsten Quadrate (englisch: Linear Weighted Least Squares) fusst.

Table of contents

Abstract **3**

Table of contents **6**

List of abbreviations **7**

Context **8**

Objective of the project **8**

Background **8**

Concept – description of the installation **9**

Procedure / Methodology **13**

Phasor Measurement Unit (PMU) 13
Phasor Data Concentrator (PDC) 13
State Estimation 18

Results **20**

Phasor Data Concentrator (PDC) 20
State Estimation 23

Discussion / evaluation of the results / lesson learnt **27**

Conclusions **28**

Perspectives, further developments **28**

References **29**

List of abbreviations

DMS	Distribution Management System
LWLS	Linear Weighted Least Squares
PDC	Phasor Data Concentrator
PMU	Phasor Measurement Unit
RTSE	Real-Time State Estimation
RTU	Remote Terminal Unit
SCADA	Supervisory Control and Data Acquisition
SE	State Estimation
WAMC	Wide-Area Monitoring and Control

Context

The progressive penetration of embedded generation in electrical distribution networks calls for the use of advanced monitoring tools able to setup a new infrastructure that allows network operators to manage the increasing complexity of these specific electrical systems. Existing Supervisory And Data Acquisition (SCADA) systems and Distribution Management Systems (DMS) use inaccurate measurements taken every few seconds or minutes that cannot accurately track the fast changes of renewable generation. Therefore, there is the need of upgrading the metering infrastructure in order to significantly enhance the performance of grid management functions that belong to two main categories: grid optimal control in normal conditions of the grid (e.g., voltage control, congestion management) and grid operation in emergency condition of the grid (e.g., fault location, isolation and service restoration).

One of the most promising technologies in this field is certainly represented by distributed monitoring systems based on the use of phasor measurement units (PMUs) that are capable of measuring the so-called synchrophasors. Within this context, this project focuses on the development of a unique PMU-based monitoring system that enables: (i) monitoring, (ii) situation awareness, (iii) control and (iv) fault management [10] in modern grids.

Objective of the project

State Estimation (SE) is a power-system situation-awareness function that computes the most likelihood state of an electrical grid (i.e., all the grid quantities: voltages, currents, powers) through the statistical processing of the measurements. The use of measurements provided by Phasor Measurement Units (PMUs) enables a very accurate, fast and frequent execution of SE, called Real-Time State Estimation (RTSE). Therefore, RTSE can improve the performance of the applications that are already using the SE output (e.g., security analysis), and it can support hard real-time applications, such as fault location and, potentially, even protections.

Our project aims at (i) validating RTSE based on PMUs in a real-scale electrical grid and (ii) demonstrating the capability of RTSE to support hard real-time applications, such as power-system protections.

Background

After the nuclear disaster in Fukushima on 11 March 2011, Switzerland, through its Federal Council, decided to phase out nuclear power. The documents "Energy Strategy 2050" and "Strategy Electrical networks: detailed concept in the context of the 2050 Energy Strategy" have been consulted and contain a package of measures for the gradual transformation of energy supply and electricity grid in Switzerland. These include the replacement of nuclear power generation through efficiency gains and the development of renewable energies. To achieve this, the power grid requires simultaneous modernization and development, including so-called intelligent techniques and an orientation towards an intelligent network (Smartgrid). The "Electrical Networks Strategy" lays down basic guidelines for these necessary transformations. Here is an excerpt:

"Increased use of measurement, information, communication and control techniques in distribution networks - also for end-users - is necessary to integrate many decentralized injections efficiently and without negative impact on security of supply".

Aware of this development, the industrial services of Lausanne have decided to familiarize themselves with a new technology and test it on their own network. This project thus provides the beginnings of a solution to an increasingly decentralized structure in which the electricity network of the future will have to demonstrate sufficient intelligence for the combined management of irregular and distributed power sources in the network and storage systems to be monitored in order to ensure secure, reliable and economical monitoring and management of the network.

Actually, the increase of RES in our distribution network becomes more and more significant in terms of installed power. As these facilities inject energy to BT and MT network, we will gradually have to extend the PMU installation in this part of our network in order to control energy and injected power. This adaptation will no doubt costly due to the dispersion of the RES in the distribution network. The use of photovoltaic cadastre of our zone of distribution can predict the architecture of the future PMU network. The creation of microgrid admitted by the strategy 2050 for the new housing areas will also require a finer management of the network, hence the need to extend the PMU in the low voltage network.

Concept – description of the installation

This section describes the characteristic of the sub-transmission grid of Lausanne as well as the technical installation of PMUs and PDC, as reported in **[1]** and **[2]**.

A schematic of the monitored portion of the 125 kV sub-transmission network of the city of Lausanne is depicted in Figure 1, which is composed of 7 buses and 10 three-phase lines. A more detailed grid schematic is depicted in Figure 2. The lines mainly consist of underground cables with two exceptions: (1) lines #8 and #10 are two parallel overhead-lines, and (2) lines #1 and #9 are two parallel lines split in two sections, i.e., they depart from bus #1 as overhead lines and after 3.682 km they go underground until bus #2.

Buses #1 and #7 are connected to a higher voltage grid through step-up transformers. At buses #2 to #6 there are step-down transformers that supply distribution networks. Moreover, at buses #1, #2 and #7 there are departing lines that link this portion of the network to the remainder of the 125 kV network. The current-flows in these lines are measured by PMUs, but these lines are not considered in this chapter. We use the current-flow measurements in these lines only to derive the power-injection measurements at buses #1, #2 and #7. No zero-injection buses are present in this network.

The monitoring infrastructure is composed of 15 PMUs that receive voltage and current signals from existing PTs and CTs installed at both ends of each line. The accuracy classes are 0.2-0.5; the rated voltage of PTs is 125 kV and the rated current of CTs is 600 A. As shown in Figure 3, PMUs consist of National Instruments Grid and Automation Systems **[3]** that implements the synchrophasor-estimation algorithm presented in **[4]**. A line breaker is present at both ends of each line and the breaker statuses are included in the PMU datagrams. Thus, we have the real-time knowledge of the network topology that is updated every 20 ms.

The full set of measurements is composed of 20 three-phase voltage phasors and 20 three-phase current-flow phasors, which leads to a redundancy level of 5.7. Such a high redundancy level was chosen in order to enable many different research studies and applications. Note that multiple voltage measurements are available at each bus. Overall, we estimate 42 state variables by using 240 measurements.

The telecommunication physical channel is the legacy optical fiber of SEL. Each substation is equipped with a switch connecting the optical fiber and the PMUs through an Ethernet cable. The communication is established through a dedicated Virtual LAN. Such a solution, among the available communication technologies for WAMC, represents the favorite one when deploying a synchrophasor network, as it enables to guarantee a fast and reliable data delivery in almost any operating condition and to exploit every feature of the PMU technology.

Each PMU is connected to a switch through an Ethernet cable and PMU data are streamed through optical-fiber to the PDC that is integrated in a workstation of the control center of SEL, which is equipped with an Intel Xeon Processor at 2.4 GHz, 8 GB of RAM and running Windows Server 2008. Synchrophasor data are streamed using the UDP protocol, as it represents the recommended protocol to deal with the high reporting rates of PMUs, by sacrificing the data reliability to the traffic speed. The PDC supplies a real-time linear state estimator of the sub-transmission grid of Lausanne, a user interface that displays in real-time both the measured and the estimated values and a local database.

PDC and SE are fully developed by the DESL of EPFL and are implemented using LabVIEW. In order to characterize the latency contributions, the PDC was equipped with a GPS receiver providing absolute time information with a resolution of 1 ms, due to the limited precision of the LabVIEW *get time* function.

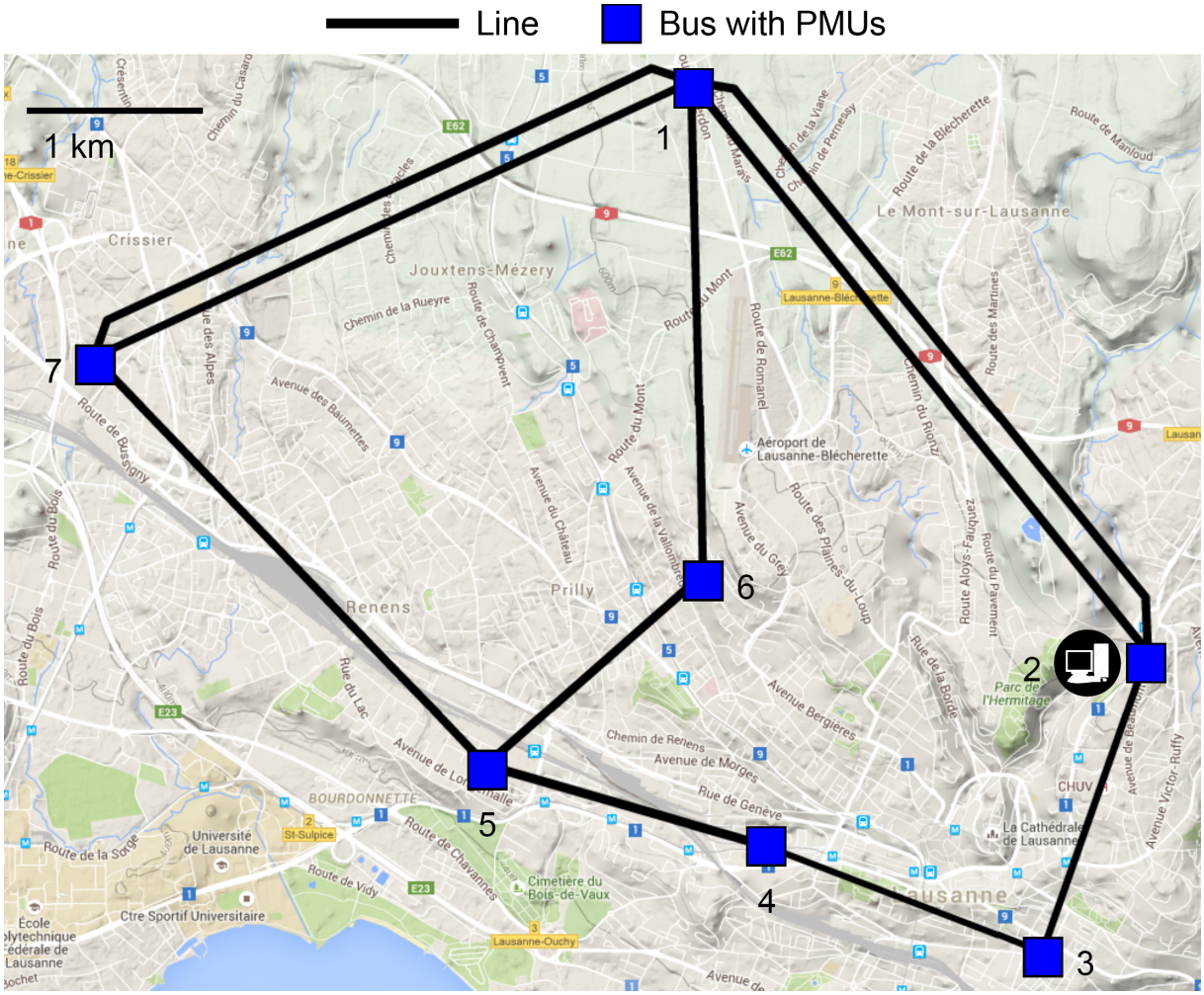

Figure 1 - Network topology of the SEL 125 kV sub-transmission grid showing the PMUs and PDC locations.

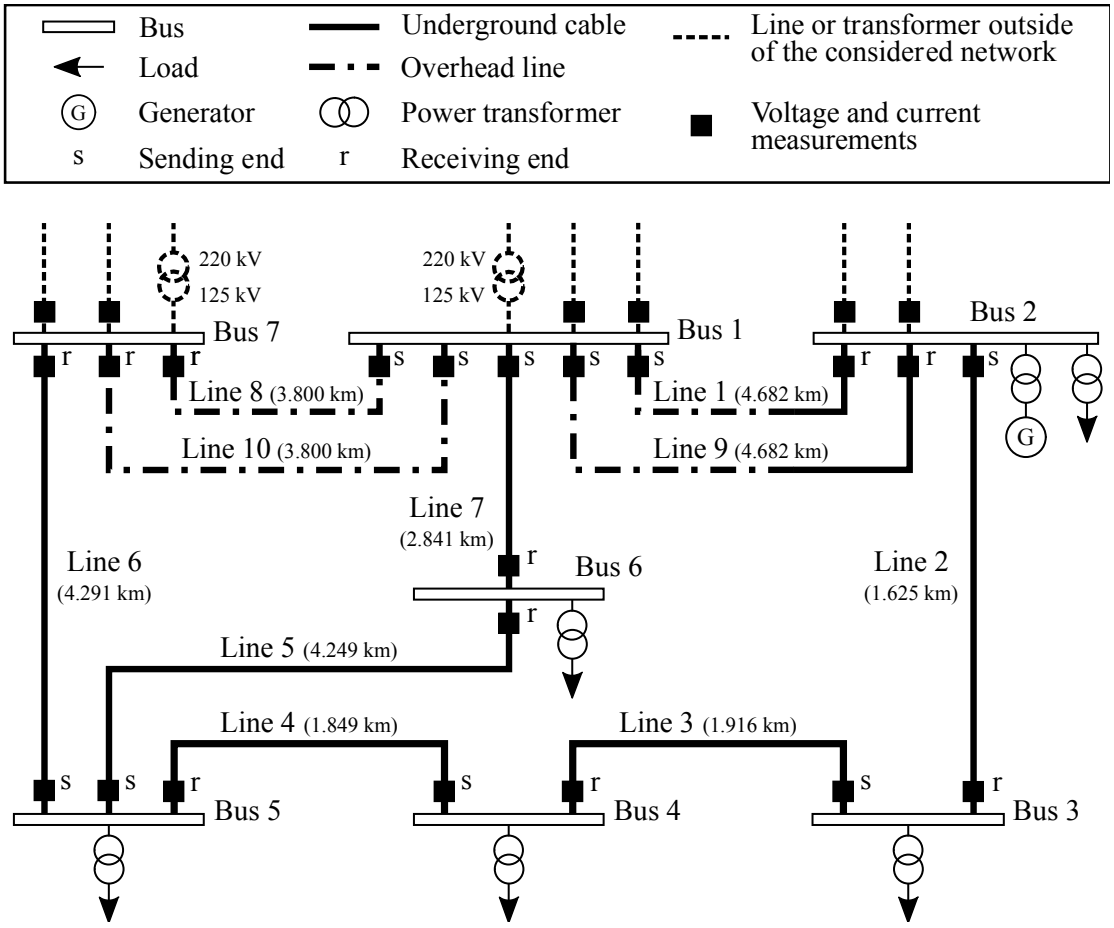

Figure 2 - Schematic of the monitored portion of the sub-transmission network of the city of Lausanne.

Figure 3 - PMU installation in an electrical substation oft he 125-kV grid of Lausanne.

Procedure / Methodology

Phasor Measurement Unit (PMU)

PMUs provide accurate and time-stamped phasors, called synchrophasors, at a typical reporting rate of 30, 50 or 60 measurements per second **[5]**. Note that PMUs measure magnitude and phase-angle of voltage/current phasors and, thus, they are capable of directly measure the power-system state. The synchronization is usually provided by the global positioning satellite (GPS) system, but can be also disseminated with dedicated communication protocols characterized by jitter below 100 ns. The PMU technology is experiencing a fast evolution triggered by the hardware-cost reduction and by the increasing requirements of several power-system applications.

The PMUs installed in the Lausanne grid are based on the National Instruments (NI) Grid and Automation Systems (GAS) **[3]** and implements the synchrophasor-estimation algorithm presented in **[4]**. This technique improves the performance of standard DFT-based algorithms by taking into account and compensating for the spectral interference produced by the negative image of the spectrum. Such a technique allows to achieve outstanding accuracy levels (Total Vector Error – TVE of 0.02%) independently of the instantaneous signal frequency and harmonic content of the input voltage/current signal. In particular, such a PMU has demonstrated to fulfill all the class-P and most of the class-M requirements defined in the IEEE Std. C37.118.1-2011.

Phasor Data Concentrator (PDC)

The Phasor Data Concentrator (PDC) is a key element of any synchrophasor network, as it is located between the various Phasor Measurement Units (PMUs) and the applications using the synchrophasor data. If not properly designed, the PDC might represent a “single point of failure” for the associated Wide-Area Monitoring and Control (WAMC) applications and eventually increase their overall latency way above the maximum allowed limits. The description of the PDC logics in the following are taken from **[6]** and **[7]**.

According to the IEEE Guide C37.244-2013 **[8]**, the most relevant functionalities of a PDC are *data aggregation* and *data pushing*, which are meant to mitigate the latency variations introduced by the various components of the synchrophasor network. Data aggregation enables to aggregate data coming from multiple PMUs into a time-aligned dataset and is typically implemented by means of a dedicated buffer. Time-alignment is not mandatory but is de-facto a standard PDC function that leverage the PMU measurement time-stamps. Data pushing enables to forward the time-aligned dataset to the subsequent applications and is typically performed by setting the so-called *PDC wait time*, i.e., the amount of time the PDC actively waits for data frames with a given time-stamp. Once the dataset is completely filled, or a maximum wait time has elapsed, the PDC pushes the dataset to the supplied applications. In **[8]** two logics are defined for setting the PDC wait time: an *absolute* time logic, where the data pushing is performed once a specific UTC time is reached, and a *relative* time logic, in which the PDC waits for a specified relative time triggered by an event, that could be the arrival of the first data with a specific time-stamp.

In general, when designing a PMU-based monitoring system, one of the main design parameters is the *PDC reporting latency*, i.e., the time difference between the instant a set of synchrophasor data characterized by the same time-stamp is pushed by the PDC to the subsequent applications and the time-

stamp itself. Depending on the supplied applications, this parameter can vary between few hundreds of milliseconds (e.g., hard real-time applications like synchrophasor-based fault management system), to few tens of seconds (e.g., soft real-time applications like voltage control).

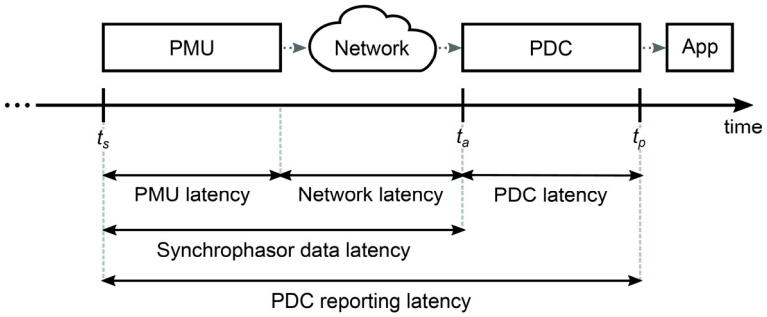

Figure 4 - The PDC reporting latency decomposed in its individual contributions. The synchrophasor time-stamp ts, the data frame arrival time ta, and the time-aligned dataset push time tp are highlighted.

The PDC reporting latency can be decomposed in its individual contributions in order to have a better understanding of the various latency sources (see Figure 4):

The *PMU measurement reporting latency* (named PMU latency in Figure 4 for sake of brevity) is defined in the IEEE Std. C37.118.1-2011 **[9]** as the time delay between the instant a specific event occurs in the power system and the instant the same event is reported by the PMU. This latency is mainly influenced by the adopted window length to estimate the synchrophasor and by the time spent in estimating the synchrophasors. It can be reduced by shortening the window length and, independently of the selected synchrophasor estimation technique, by adopting more performing hardware platforms. However, such a contribution turns out to be quite deterministic compared to others.

The *communication network latency* is the time difference between the instant a PMU has transmitted a data frame on its physical channel and the instant the same data frame hits the PDC network interface. Together with the PMU measurement reporting latency, it defines the so-called *synchrophasor data latency*. Synchrophasor data can be carried over any wired or wireless communication layer that has sufficient bandwidth and reduced data transmission latency to support PMU data streams characterized by a specific reporting rate and message size. Depending on the adopted information and communication technology, this contribution might introduce relatively high delays and non-deterministic latency variations.

The *PDC latency* is defined as the time difference between the instant a time-aligned dataset is pushed to the supplied applications and the instant the first message with a given time-stamp hits the PDC. The PDC latency is composed of two contributions: (i) the PDC wait time that starts when the first message with a specific time-stamp enters the PDC and ends when the last one arrives or the associated timeout expires; (ii) the PDC processing time, i.e., the amount of time needed by the PDC to complete the production of an aggregated dataset. Typically, the former by far outweighs the latter. It is worth pointing out that a well-designed PDC does not introduce any latency: it simply acts as a buffer that mitigates the real-time variation of the synchrophasor data latency, by waiting the necessary amount of time to gather most of the incoming data frames characterized by the same time-stamp. Reference **[8]** does not define a specific limit value to the PDC latency, it just emphasizes the fact that it should be as low as possible, coherently with the PDC wait time setting.

A high-level design of the proposed PDC architecture is shown in Figure 5. It implements most of the functions described in **[8]**. However, for the sake of brevity, we focus only on those affecting the PDC reporting latency and the data incompleteness.

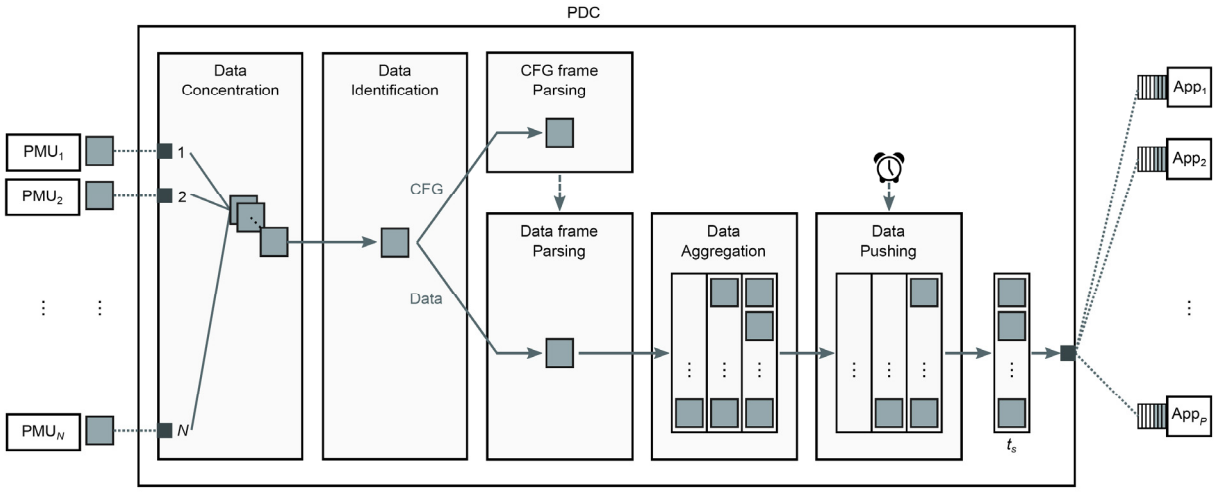

Figure 5 - Architecture of the proposed PDC collecting data frames from N PMUs and pushing time-aligned datasets to P applications.

For each connected PMU, the PDC opens a socket (UDP or TCP) on a specific local port and continuously listens to incoming PMU data frames. When a new datagram is received, data validation is performed and invalid frames are discarded. The frame follows a different path based on its type. Once the configuration frame for a given PMU is received, the parsing of data frames coming from that specific PMU can start (as it is known, configuration frames enable the PDC to interpret the data frames). Finally, the PDC time-aligns the data and pushes the aggregated dataset to the supplied applications.

To accomplish the data aggregation and data pushing functions, a circular fixed-size data buffer is adopted (see Figure 6). The buffer is implemented as a 2D array, having columns, one for each PMU, and M rows, one for each stored time-stamp. During the initialization phase, a specific column of this buffer is assigned to each PMU data stream, based on the stream IDCODE, a number that identifies a specific PMU data stream.

The number of rows M is hereafter called buffer depth and represents the amount of time-stamps that are stored in the buffer. The buffer history length T_h can be derived from the buffer depth and the PMU reporting rate as $T_h = M/F_r = M*T_r$, being $F_r=1/T_r$ the PMU reporting rate and T_r the PMU reporting interval. Each row represents a time-aligned dataset gathering data frames with a specific time-stamp t_s from all PMUs. A pointer points to the next line to be pushed to real-time applications. The line order is such that time-stamps are monotonically increasing within the circular buffer. When the buffer is filled new data overwrites the old one. This avoids to rotate the buffer's elements when data are released.

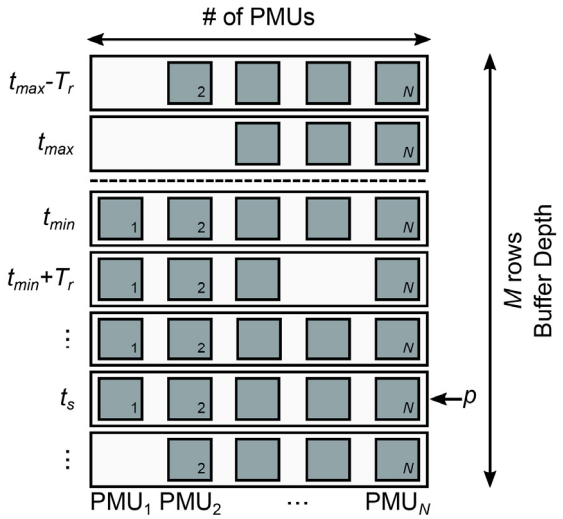

Figure 6 - Layout of the circular buffer used to aggregate and time-align the incoming data flows generated by N PMUs. It can store up to M time-aligned datasets characterized by time-stamps in the range $t_{min}<t_s<t_{max}$. A pointer p points the next line to be pushed to the supplied applications.

Stand-alone logic for Data Aggregation

In the developed PDC, data aggregation is performed with time-alignment. A new data frame is filled in position (m,n) of the buffer, being □ the buffer line corresponding to its time-stamp t_s and n the column corresponding to its PMU ID.

Before inserting the data frame in a specific buffer position (m,n) the buffer lines are updated depending on the received time-stamp t_s unless $t_s<t_{min}$, in which case the data frame is discarded. If $t_{min}<t_s<t_{max}$ the buffer time-stamps are not updated. If $t_s>t_{max}$, the oldest lines are first fed to soft real-time applications and then replaced with the newest ones. In this case, starting from the line characterized by the minimum time-stamp t_{min}, a set of $\frac{t_s-t_{max}}{T_r} \in \mathbb{N}$ empty lines, characterized by newer time-stamps up to ts, overwrites the older ones. If a data-frame characterized by a time stamp greater than the actual UTC time is received (i.e., a time-stamp coming from the future), the data frame is discarded. This plausibility check is possible only by synchronizing the PDC to an absolute time reference.

Such a data aggregation logic, that overwrites older lines whenever a newer time-stamp is received at the PDC, gathers data frames independently of the adopted data pushing logic without causing any memory leak.

Absolute and Relative Time Data Pushing logics

In order to present a possible implementation of the absolute and relative time data pushing logics, let us consider the aggregation process of data frames characterized by time-stamp t_s coming from a set of N PMUs (see Figure 7). Let us also assume that the arrival times of the first and last data frames hitting the PDC are $t_{a,i}$ and $t_{a,j}$ respectively, i.e., the arrival times of the data frames generated by the i-th and j-th PMUs.

In case an absolute time data pushing logic is adopted, the PDC must be synchronized to an absolute time reference. The wait time refers to the data frames time-stamp ts and elapses at time tp=ts+Tabs being tp the PDC push time and Tabs the absolute PDC wait time.

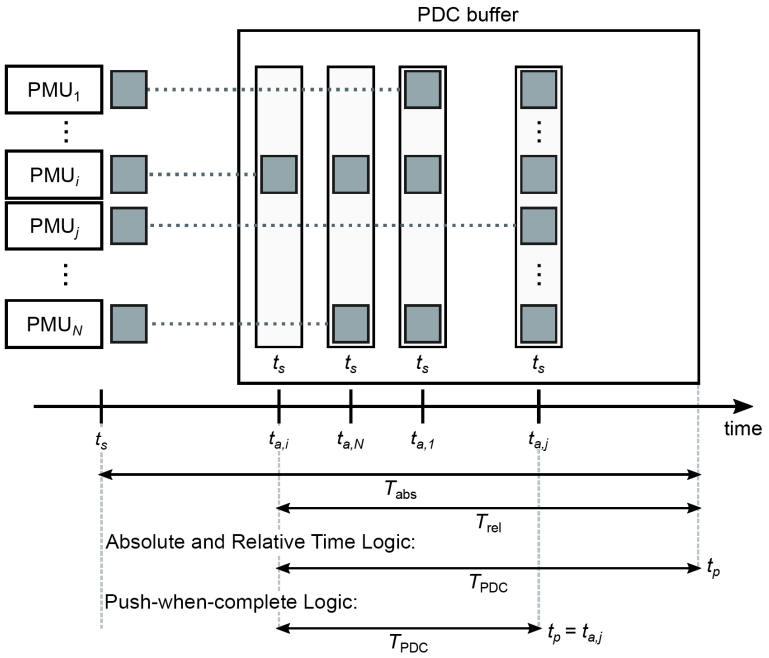

Figure 7 - Comparison between the various data pushing logics in the case of a PDC gathering data frames from N PMUs characterized by time-stamp t_s. The arrival times of the first and the last data frame characterized by time-stamp t_s are indicated by $t_{a,i}$ and $t_{a,j}$, respectively.

Besides, in case a relative time data pushing logic is adopted, the wait time counter is triggered by the reception of the first data frame characterized by a time-stamp t_s and elapses at time $t_p=t_{a,I} + T_{rel}$, being T_{rel} the relative wait time. It is evident that adopting a relative time data pushing logic might not always guarantee to fulfill the latency requirements of the supplied application, which might be affected by the real-time variations of the network latency (i.e., the jitter of the inter-arrival times).

At time t_p the aggregated dataset is pushed to the supplied applications and the pointer p is incremented (modulo the buffer depth M). The introduction of the pointer p guarantees that, even if data frames arrive in the PDC out of order, the time-aligned datasets are always pushed based on the time-stamp order.

For both absolute or relative time data pushing logics, when the wait time has elapsed, the time-aligned dataset is pushed even if some data have not yet reached the PDC and the missing data is indicated by rising a proper flag. In such a case, the subsequent applications are assumed to cope with incomplete datasets by using replacement techniques or historical information. Consequently, a delayed packet that reaches the PDC when its corresponding dataset has already been pushed, is lost and it is no longer available for further applications.

Even though this report does not deal with the optimal selection of the PDC wait time, it is evident that this parameter plays a crucial role in the overall PDC design. It must be selected as a trade-off between the desired dataset completeness and the latency requirements of the power system application being

served by the PDC. In case of non real-time applications, to reduce dataset incompleteness due to late data arrival, longer PDC wait times can be set, with the consequent increase of the overall latency of the system. Such an approach cannot be adopted for real-time applications and the PDC wait time must be set accordingly. In the case of absolute time logic, T_{abs} has to be set according to the measured synchrophasor data latency in order to push time-aligned datasets that are mostly complete. In this case the minimum allowed buffer depth is

$$M = \left\lceil \frac{T_{abs} - T_{min}}{T_r} \right\rceil + 1$$

where $\lceil \cdot \rceil$ represents the ceiling function and T_{min} the minimum possible PMU measurement reporting latency. Besides, in case of relative time, T_{rel} has to be set according to the measured time needed to receive all data frames of a specific dataset. The resulting minimum buffer length is computed as

$$M = \left\lceil \frac{T_{rel}}{T_r} \right\rceil + 1$$

As the same PDC can simultaneously supply applications characterized by different time requirements, several instances of the presented data pushing logics can run in parallel on the same buffer. Each one has its own PDC wait time setting and its own pointer p. In such a case, the actual buffer depth M is defined by the maximum PDC wait time. Therefore, the data aggregation process in a buffer line that has already been pushed to a hard real-time application continues until the limit allowed by the buffer depth. Consequently, datasets that are more likely to be complete are fed to soft real-time applications (for instance, a local database).

Push-when-complete logic

If the synchrophasor network is properly designed and the PDC wait time correctly set, most of the datasets are completed before the timeout elapses. According to the logics presented so far, these datasets would keep on waiting in vain for the wait time to elapse before being pushed. In this respect, a consistent approach would push the dataset once it is complete regardless of the wait time. The majority of the datasets will be then pushed according to this logic, unless data frames are lost or delayed. In such a case the absolute or relative time logics would take over and push uncompleted datasets once the PDC wait time has elapsed. Such a logic has the main advantage of minimizing the PDC reporting latency, that is reduced to the synchrophasor data latency of the latest received data frame, and enables to increase the time budget allocated for the other functionalities. On the contrary, the main drawback of such an approach is that the data pushing time tp varies based on the data frames arrival time. Hence, the supplied applications should be designed in order to properly cope with non-deterministic datasets arrival. In this respect the easiest solution is to embed dedicated FIFO (First-In-First-Out) data structures in each one of the supplied applications, in order to take care of the non-deterministic synchrophasor data latency.

State Estimation

The SE theory reported in this section is taken from the PhD thesis of Lorenzo Zanni **[1]**.

A fundamental application that is fed by PDC data is SE. In general, the state of a power system refers to the minimum set of independent variables from which all the power-system quantities (voltages, current/power flows/injections, etc.) can be computed. This is why the state fully defines the power-system

operating conditions. In this report, the state always refers to the so-called static state that is typically defined as the set of nodal phase-to-ground voltage phasors at all network buses.

The knowledge of the state is fundamental in the operation of the transmission system as it is required by several functions, such as security control and economic dispatch. Therefore, the procedure that infers the power-system state has to be accurate and reliable.

Traditionally, SE is supplied with measurements provided by Remote Terminal Units (RTUs) that consist of voltage/current magnitudes and power flows/injections, which are commonly called conventional measurements or SCADA measurements. The availability of this type of measurements has led to the development of state estimators with the following characteristics:

1. The estimation algorithm is non-linear and iterative due to the non-linearity of the function that links power and current-magnitude measurements to the voltage state-variables;

2. The refresh-rate is in the order of tens of seconds or minutes due to the low acquisition-rate of RTUs and the high-computation time of the SE algorithm;

3. RTU measurements are usually not time-stamped or are time-stamped with poor accuracy (not sub-second); in the former case, they are time-stamped in the SCADA by inferring the delay added by both RTU processing and telecommunication network. Therefore, the time-skew between measurements can introduce significant and unknown errors in the estimated state;

4. One of the buses has to be chosen as the reference bus for the voltage phase-angle that is fixed to an arbitrarily selected value (usually equal to zero) at this bus.

As PMUs start populating the network, in some portions of the grid the observability and redundancy requirements are matched only with PMUs. The fact that the state of these portions of the grid can be estimated by using exclusively synchrophasor measurements leads to a remarkable improvement of the SE performance.

The main benefits for SE relying only on this type of measurements are listed here below:

1. When only voltage and current phasors are used, the equations linking measurements and state variables, called measurement model, are linear. Therefore, we can employ linear SE that is not iterative and characterized by lower computational time, increased numerical stability and no approximations in the measurement model;

2. Each synchrophasor measurement is time-stamped and its phase-angle is aligned. Hence, the measurements can be phase-aligned at the data collection point, even if they are received at different time-instants. This ensures a superior accuracy of the SE solution, as the set of measured phasors is coherent with respect to time;

3. The very high PMU reporting-rate leads to a SE process characterized by high refresh-rate and low latency, which is typically called RTSE;

4. As PMUs directly measure the phasor phase-angle, we do not need to choose a reference bus where the voltage phase-angle is fixed. All the phase-angle measurements are processed at the same time by the state estimator.

Besides, a PMU measures the phasors in each of the three phases, so that we can use three-phase SE. The advantage consists in the possibility to account for network parameter asymmetries and for imbalances in the network operating-conditions.

For the SE of Lausanne grid, we employed the linear weighted least squares (LWLS) algorithm. The LWLS is a widely-used state estimator for power systems, as it is characterized by fast computational speed and simple implementation. It is a static estimator as it does not exploit any time-variant dependency of either the measurements or the state variables. Let us define the linear measurement model that relates the measurements to the state variables, which is

$$\mathbf{z} = \mathbf{H}\,\mathbf{x} + \mathbf{v}$$

where **z** is the measurement vector, **x** is the state vector, **v** is the measurement noise, and **H** is the matrix linking **z** and **x**. The measurement noise is assumed to be white and Gaussian with covariance matrix **R**.

The LWLS relies on the following assumptions:

1. The measurement noise is Gaussian-distributed with mean value equal to zero.
2. The measurements are uncorrelated, so that **R** is diagonal.
3. Matrix **H** is of full rank, which means that the network is observable.

The LWLS minimizes the sum of the squared residuals weighted by the measurement variances, a residual being the difference between the measurement and the fitted value obtained with the model. Thanks to the use of PMUs, the measurement model is linear and the LWLS optimization problem has a closed form solution that is very fast to compute. Thus, SE can be computed in real-time even at the same PMU measurement reporting-rate.

Results

Phasor Data Concentrator (PDC)

In this section, the considered PDC logics are compared and the results are taken from **[6]**. For the time-latency assessment, the data flow was tracked along the whole process (from PMUs to PDC) by measuring the data frame time-stamp ts, their arrival times ta and the PDC push tim tp. The synchrophasor data latency of each data frame and the PDC reporting latency of each time-aligned dataset were computed for several data pushing logics. In particular, four different data pushing logics were examined over an observation window of 24 hours:

1. Absolute time logic (hereafter referred as Logic 1);
2. Absolute time integrating push-when-complete logic (hereafter referred as Logic 2);
3. Relative time logic (hereafter referred as Logic 3);
4. Relative time integrating push-when-complete logic (hereafter referred as Logic 4).

The experimental results are presented by means of three histograms representing the probability density function (PDF) of the following quantities:

a. the aggregated synchrophasor data latencies from all PMUs;

b. the comparison between the PDC reporting latency in Logics 1 and 2;

c. the comparison between the PDC reporting latency in Logics 3 and 4.

Also, for each data pushing logic, the dataset incompleteness is presented by means of a table showing the percentage of incomplete datasets pushed by the PDC during the 24 hours observation window. In order to properly set the PDC wait time, a preliminary test was performed to measure the characteristic synchrophasor data latencies together with their jitter over a time window of 24 hours. This quantity has then been set to guarantee the collection of the majority of the data frames with a particular time-stamp, independently of the adopted data pushing logic.

The experimental results are presented in Figure 8. Both the absolute and relative PDC wait time were set by analyzing the aggregated synchrophasor data latencies from all PMUs measured along an interval of 24 hours, as shown in Figure 8a. The histogram represents the aggregated data, because an analysis by PMU data stream showed no significant differences among the various PMUs. As it can be noticed, they are characterized by a mean value of 44 ms and standard deviation of 2 ms. Nevertheless, as more than 99.99% of the packets is received with a latency smaller than 60 ms, the absolute PDC wait time was set to this value. Besides, the average amount of time needed to receive all data frames with specific time-stamp is 3 ms, whereas more than 99.99% of datasets takes less than 20 ms to complete. Hence, the relative PDC wait time was set to 20 ms. The comparison between Logics 1 and 2 (see Figure 8b) shows the improvement introduced by adopting the push-when-complete logic, that enables to reduce the PDC reporting latency by 14 ms. Nevertheless, the latter increases the jitter of the PDC reporting latency that is less deterministic compared to Logic 1 as it is always influenced by the arrival time of the last-received data frame with a specific time-stamp. The push-when-complete logic also reduces the PDC reporting latencies when adopting a relative time data pushing logic, with an average improvement of 15 ms (see Figure 8c comparing Logics 3 and 4). In such a case the PDC reporting latency jitter is slightly improved by adopting Logic 4 but it is still non-deterministic as in case of Logic 1.

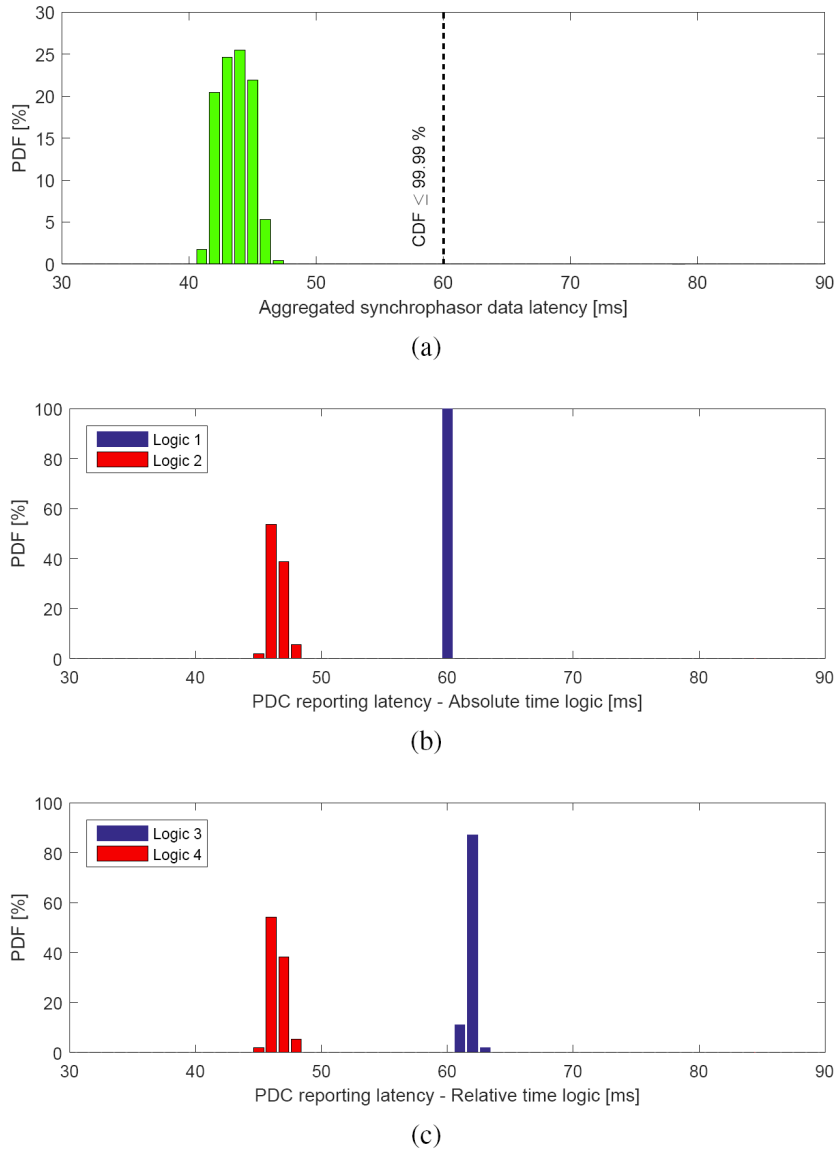

Figure 8 - Experimental results in the SEL field trial showing the PDF of: (a) the combined synchrophasor data latencies; (b) the PDC reporting latency when adopting an absolute time logic (Logic 1) and when integrating it with a push-when-complete logic (Logic 2); c) the PDC reporting latency when adopting a relative time logic (Logic 3) and when integrating it with a push-when-complete logic (Logic 4).

	% of incomplete datasets			
Missing data frames	Logic 1	Logic 2	Logic 3	Logic 4
1	$2.3{\cdot}10^{-5}$	$2.3{\cdot}10^{-5}$	0	0
2	0	0	0	0
3	$6.8{\cdot}10^{-5}$	$6.8{\cdot}10^{-5}$	$4.5{\cdot}10^{-5}$	$4.5{\cdot}10^{-5}$
>3	$1.5{\cdot}10^{-3}$	$1.5{\cdot}10^{-3}$	$5{\cdot}10^{-4}$	$5{\cdot}10^{-4}$
Total	$1.6{\cdot}10^{-3}$	$1.6{\cdot}10^{-3}$	$5.4{\cdot}10^{-4}$	$5.4{\cdot}10^{-4}$

Figure 9 - Dataset incompleteness when adopting different data pushing logics in the SEL field-trial.

Based on the adopted PDC wait time setting (T_{abs}=60ms, T_{rel}=20ms), the incompleteness of the time-aligned datasets is presented in Figure 9. As expected, when transmitting data frames through a dedicated wired telecom infrastructure, the dataset incompleteness is negligible and in the order of few parts per million regardless of the adopted data pushing logic. Nevertheless, occasionally the PMU data frames are simultaneously delayed by a considerable amount of time and do not reach the PDC before the expiration of the absolute PDC wait time. This causes the PDC to push empty data-sets in case of Logics 1 and 2, yielding to a total data-set incompleteness that is one order of magnitude higher compared to Logics 3 and 4.

State Estimation

The analysis of the SE results is taken from the PhD thesis of Lorenzo Zanni **[1]**.

We consider a 100 s time window of measurements taken in a summer day at 10 a.m. (Swiss local time) where the network is in quasi-static conditions as there are no particular events taking place.

A snapshot of the grid operating-conditions is presented in Figure 10, Figure 11 and Figure 12, which includes the measurements taken at time-step 1 of power-injections, sending-end power-flows and receiving-end power-flows, respectively (power measurements are derived from voltage and current phasors). In Figure 11, we can observe the presence of not negligible active-power flow unbalances among the phases (e.g., almost 1 MWdifference between phases a and b of line #2) and between the two parallel lines #1 and #9 (about 300 kW in phase c). The same unbalances are present also at the receiving-ends, which proves that they are not due to measurement errors. This phenomenon is even more evident in the reactive-power flows (e.g., almost 1MVAR difference between phases a and c of line #2). These considerations underline the importance of a three-phase state estimator. Comparing Figure 11 and Figure 12, it can be seen that sending- and receiving-end active-power flows are consistent, which allows us to qualitatively presume that no gross measurement-errors are present.

Figure 13 shows the voltage measurements and LWLS estimates at all the buses at time-step 1. The relative voltage drop between buses is quite small as all the voltages lie in a range of 0.001 pu; this is justified by the low reactive power flows. On the contrary, higher active-power flows result in larger phase-angle separations in the order of a few milliradians. However, both voltage magnitude and phase-angle variations are small due to the stiffness of this grid. The mismatch between measured and estimated values is constant in time, because it is due to the systematic errors of the PTs. The random measurement-noise is again very small and can be disregarded.

The power-flow measurements are taken in all the lines departing from each bus (even in the interconnection lines departing from buses #1, #2, #7, which are external to the considered network). Therefore, we can compute the sum of all the active-power flows, which represents the grid losses. In

Figure 14 we show the measured and estimated grid losses as well as the total reactive power produced by the transmission lines. Considering that the measured values contains the sum of the errors of all the measurements, a difference of about 100 kW between estimated and measured values can be considered a small error due to PT and CT inaccuracies. Therefore, this result quantifies the qualitative consideration regarding the absence of gross measurement-errors that we drew by comparing Figure 11 and Figure 12. The total grid losses (about 100kW) are very small compared to activepower flows, whereas the reactive power produced by the transmission lines is much larger than the reactive-power flows as they mainly consist of underground cables.

Figure 15 displays the distributions of the LWLS normalized residuals for the considered 100 s time window. All the voltage measurements can be considered to be correct as their normalized residuals are below the selected threshold for bad-data identification, which is equal to 4. However, the majority of the normalized residuals related to current-flow measurements (both at the sending- and receiving-ends) are much larger than 4 and reach values up to 40. We can further comment that the high normalized residuals are not outliers that occurs once in a while, because they have median values up to 25. The classic cause of normalized residuals that are systematically large is network-model errors. As we are sure about the correctness of the topology, the main suspects are the line parameters. We exclude measurement errors as possible cause, because sending- and receiving-end current-flow measurements are coherent and the total power balance derived from the measurements is in agreement with the estimated one. Investigations on this theme are ongoing.

However, although these normalized residuals may appear quite high, we should remind that current-flow measurements are very sensitive to line-parameter errors. Indeed, if we carry out the same simulation by using only voltage and current-injection measurements (the current injections can be computed from the current-flows by means of the Kirchhoff's law, because we measure all the current-flows departing from each bus), all the normalized residuals fall below 2. In addition, the difference between measured and estimated currents expressed as a percentage of the current magnitudes is always below 6 %, which is acceptable.

Bus #	#1	#2	#3	#4	#5	#6	#7
$P_{inj,a}$ [MW]	32.214	-18.307	-6.400	-9.108	-8.033	-5.576	15.262
$P_{inj,b}$ [MW]	32.276	-18.814	-6.221	-8.764	-7.703	-5.274	14.592
$P_{inj,c}$ [MW]	32.837	-19.287	-6.335	-8.895	-7.913	-5.359	15.047
$Q_{inj,a}$ [MVAR]	-3.337	0.343	-1.406	-2.376	0.005	-1.081	1.845
$Q_{inj,b}$ [MVAR]	-3.943	0.981	-1.510	-2.477	-0.029	-1.224	2.236
$Q_{inj,c}$ [MVAR]	-3.462	-0.079	-1.209	-2.104	0.328	-0.955	1.467

Figure 10 - Power-injection measurements at time-step 1.

Line #	#1	#2	#3	#4	#5	#6	#7	#8	#9	#10
$P_{s,a}$ [MW]	10.739	3.008	-3.406	-12.526	-6.043	-14.513	-11.596	-0.358	10.611	-0.373
$P_{s,b}$ [MW]	10.532	2.131	-4.099	-12.862	-6.126	-14.437	-11.411	-0.064	10.450	-0.053
$P_{s,c}$ [MW]	10.670	2.281	-4.060	-12.977	-6.370	-14.518	-11.729	-0.250	10.937	-0.249
$Q_{s,a}$ [MVAR]	-0.105	0.456	-0.450	-2.184	-0.067	-1.569	-0.951	-0.881	-0.519	-0.880
$Q_{s,b}$ [MVAR]	-0.770	0.563	-0.421	-2.249	0.058	-1.815	-0.920	-0.944	-0.382	-0.927
$Q_{s,c}$ [MVAR]	-0.705	-0.490	-1.182	-2.653	-0.128	-1.669	-1.022	-0.637	-0.446	-0.652

Figure 11 - Power-flow measurements at the sending-ends of the lines at time-step 1.

Line #	#1	#2	#3	#4	#5	#6	#7	#8	#9	#10
$P_{r,a}$ [MW]	-10.717	-2.994	3.418	12.523	6.042	14.532	-11.618	0.358	-10.598	0.372
$P_{r,b}$ [MW]	-10.513	-2.122	4.097	12.860	6.141	14.464	-11.415	0.058	-10.432	0.069
$P_{r,c}$ [MW]	-10.652	-2.275	4.082	12.974	6.376	14.550	-11.736	0.249	-10.916	0.248
$Q_{r,a}$ [MVAR]	-0.266	-0.956	-0.192	1.642	-1.160	0.196	0.079	0.813	0.153	0.836
$Q_{r,b}$ [MVAR]	0.398	-1.088	-0.228	1.728	-1.276	0.456	0.052	0.884	0.020	0.896
$Q_{r,c}$ [MVAR]	0.334	-0.027	0.549	2.124	-1.107	0.299	0.152	0.575	0.076	0.593

Figure 12 - Power-flow measurements at the receiving-ends of the lines at time-step 1.

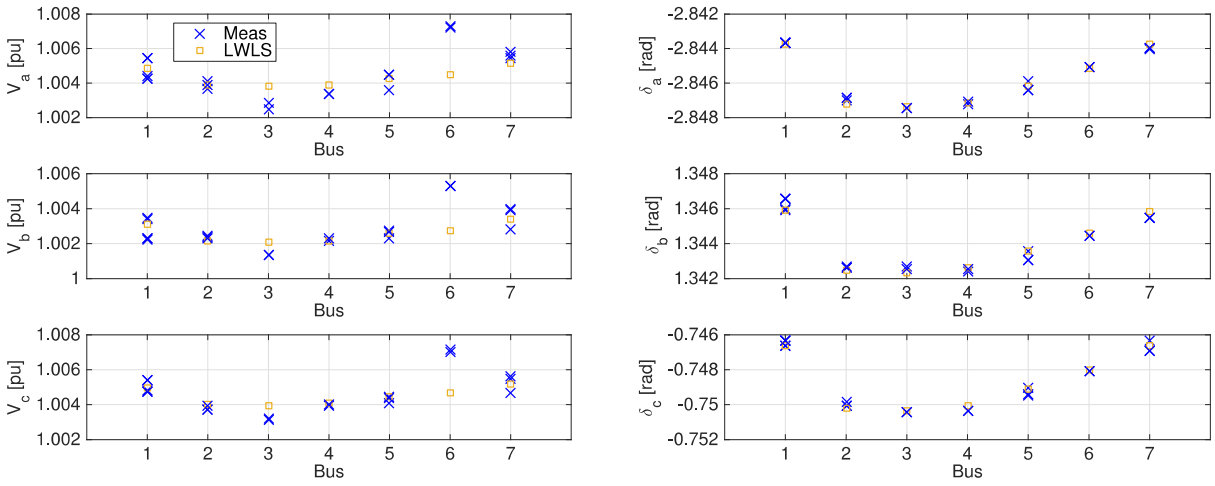

Figure 13 - Voltage magnitude and phase-angle at time-step 1.

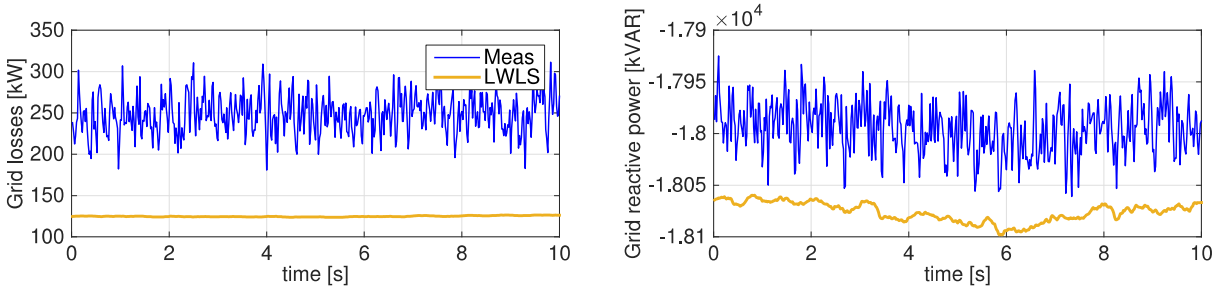

Figure 14 - Time evolution of the total grid losses and of the total reactive power produced by the transmission lines.

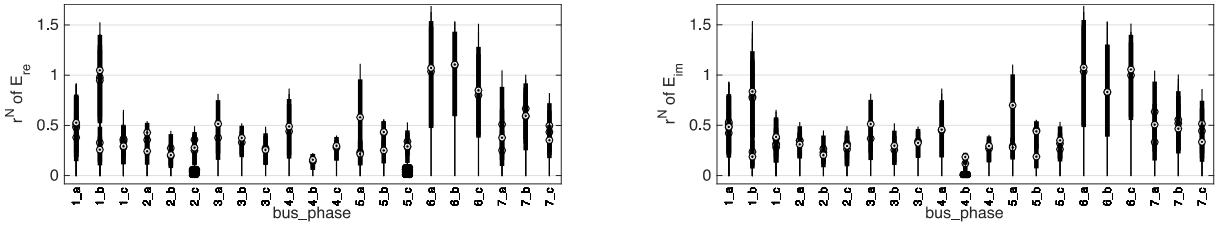

(a) Real and imaginary parts of the voltage measurements.

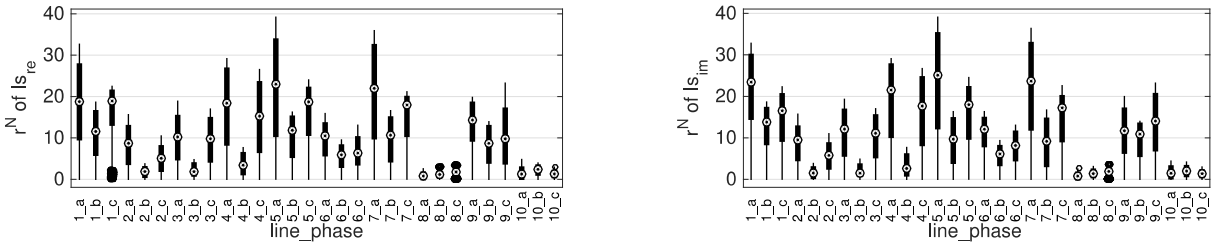

(b) Real and imaginary parts of the sending-end current-flow measurements.

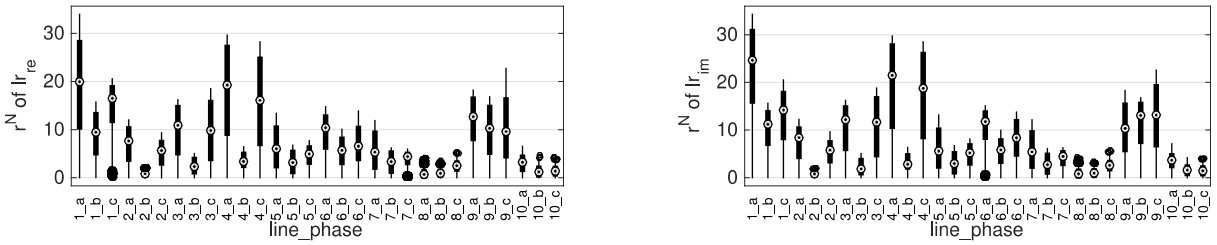

(c) Real and imaginary parts of the receiving-end current-flow measurements.

Figure 15 - Statistics of the distributions of the normalized measurement-residuals of the LWLS.

We did not only analyze the measurements of PMUs, but we wanted to provide a useful tool for the operators of SEL. Therefore, we developed a Graphical User Interface (GUI) that is shown in Figure 16. This GUI displays in real-time the electrical quantities that the operators of SEL need to constantly monitor, such as power flows and voltages. The data of this GUI are updated once a second, which is around 1000 times faster than the refresh rate of the SCADA system, which is in the order of 15 minutes.

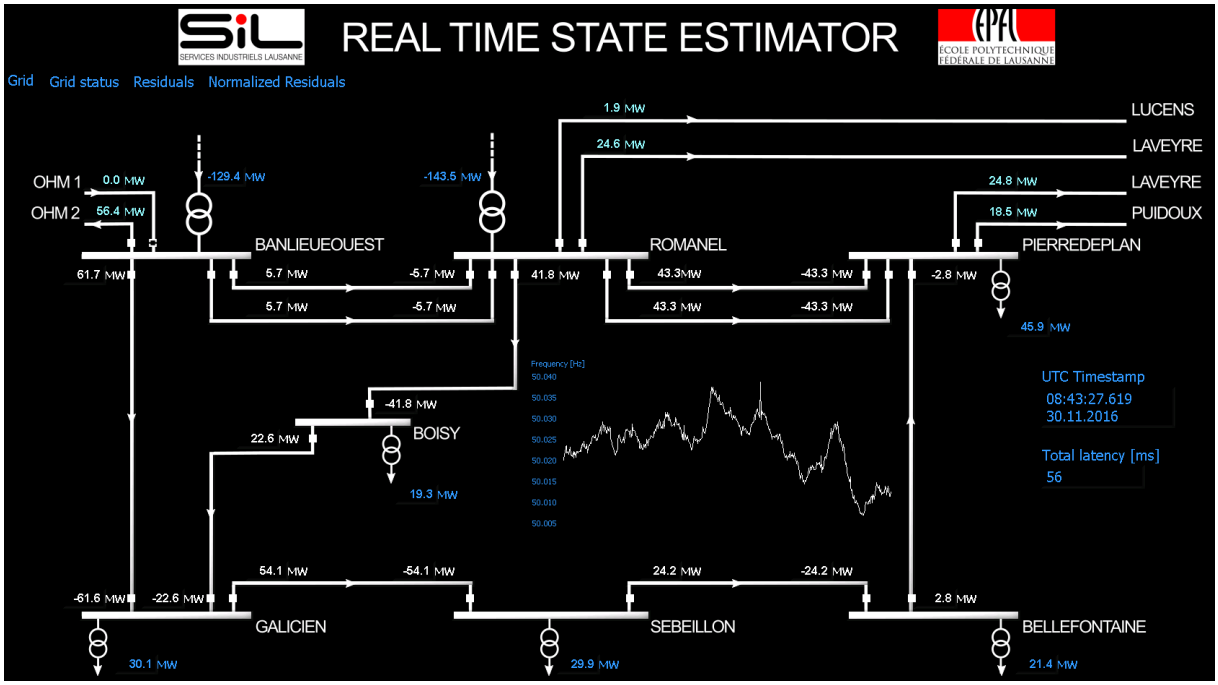

Figure 16 - Graphical user interface for the operators of SEL.

Discussion / evaluation of the results / lesson learnt

The results reveal the correct implementation and operation of the entire system composed of PMUs, fiber-links telecommunication network, PDC and SE.

We have tested in the real filed the effects of different data puhsing logics on the overal SE latency. In particular the experimental validation has demonstrated that the push-when-complete logic is characterized by the lowest PDC latency (4 ms on average), which is only influenced by the synchrophasor data latency. Nevertheless, the latency reduction introduced by this logic involves a reduced determinism of the outgoing PDC data flow. As a consequence, in order to correctly operate, this logic has to be properly coupled with dedicated FIFO structures to mitigate the variations in the PDC reporting latency.

On the other hand, the only logic that, independently of the network characteristics, is capable of guaranteeing a constant PDC reporting latency and the consequent mitigation of the synchrophasor data latency variations is the absolute one. In such a case, the PDC reports time-aligned datasets at a constant reporting rate (corresponding to the PMU one) with a PDC reporting latency that is fixed and coincides with the absolute PDC wait time. In such a case, the average PDC latency is 16 ms.

The SE has little deviations from the PMU measured values, showing that it is correctly implemented. These deviations are due to small line-parameter errors as line-flow current measurements are particularly sensitive to parameter errors in a meshed grid that is not heavily loaded. However, the use of the estimated state instead of the raw measurements is still the best choice, because SE can guarantee the filtering of gross errors.

Besides, this complex systems is remarkably stable as is runs 24/7 and we experienced only few software crashes.

The SEL operators are still constantly using the developed GUI to verify the data displayed by their SCADA. This GUI ca be used as a backup of the SCADA system: if the SCADA shut down for some unforeseen reasons, this GUI could become vital to keep the control of grid operation.

In addition, the much higher refresh-rate of the developed GUI with respect to the SCADA system can be important in emergency conditions, when quick decisions have to be taken based on the grid state.

Conclusions

At present, most of the distribution networks are managed using conventional operating systems (SCADA). It is difficult to predict how rapidly changes will have to take place so that operators have more efficient means. Nevertheless, it is certain that an evolution will take place over the next few years due to the increase in decentralized energy production, the storage that will be increasingly associated with it, and consumer groupings with self-production. Network management models will need to be updated to ensure interconnection, synchronization and continuity of energy supply. Management will become more complex and will require, among others, a more detailed view of what is going on in the distribution network, that the PMU allows.

The results of this project are notable because they have made it possible to test and demonstrate the correct functioning of the state estimator developed by the DSEL in a high voltage distribution network. In addition, we have also verified the accuracy of the fault locator [10], a very useful tool for the network operator. The difficulties encountered in the integration of PMUs and their networking have been easily controlled thanks in particular to the performance of the fiber optic network of the City of Lausanne.

A very important aspect in the success of such a project is the collaboration between the various stakeholders: researchers from the DESL, the PWRS, the Organization and Informatics Service of the City of Lausanne and the engineering and SEL technicians. All these entities and individuals have worked to achieve a successful combination of theory and practice.

Perspectives, further developments

When will the distribution system operator decide on total control and control by a PMU network?
The level of security that an operator must set is such that this change will take time because human and technical adaptation is still necessary to trust in a new operating system. SIL will continue to use the state estimator and the PMU network in parallel with its SCADA system to use it as a complementary tool in the management of its distribution network.

What is the interest today to have a real time state estimator for a GRD ?
Added value for the management of our network at 125 kV is interesting, however it remains modest. In fact the quality and the reliability of the measurements obtained with a SCADA is already very high and allows us to effectively control our high voltage network.

However, this project helped validate on a real network a concept and technologies for estimating the state of this with a refresh rate of 20 ms and this result is remarkable.

The disadvantage is the fact that costs in equipment hardware, software and human to deploy to achieve this are still very high compared to the added value obtained. There is no doubt that in having validated this methodology in the real conditions, he will follow technical developments and a scale effect that will make it less in medium-term.

The most attractive prospect is able to deploy this technology on the medium and low voltage networks, which should lead to better monitoring these networks with an overall cost which should be less than what could be obtained with a SCADA because there might be fewer points of measurements in real time. If an ergonomic function for default location can be integrated, added value will be great as currently it is tedious to locate defects in these voltage levels. This development is beyond the scope of this project but the first step is already been crossed.

For the next step, the intention of the SIL is to extend this experiment in a sensitive part of its medium and low voltage network in order to get closer to decentralized production facilities. This stage began in early 2017 with the collaboration of Zaphiro Technologies, a startup company recently created by tree DESL researchers.

References

[1] Lorenzo Zanni, Power-System State Estimation based on PMUs: Static and Dynamic Approaches – from Theory to Real Implementation. PhD thesis, EPFL, 2017.

[2] Asja Derviskadic, Development of a PMU-based real-time state estimation of sub-transmission networks: theory and experimental validation based on the Lausanne 125 kV grid. Master thesis, Università di Roma, 2015.

[3] “National Instrument Grid Automation System.” http://www.ni.com/white-paper/52556/en/. Accessed: 2016-09-08.

[4] P. Romano and M. Paolone, “Enhanced interpolated-DFT for synchrophasor estimation in FPGAs: Theory, implementation, and validation of a PMU prototype,” Instrumentation and Measurement, IEEE Transactions on, vol. 63, pp. 2824–2836, Dec 2014.

[5] P. System, R. Committee, I. Power, and E. Society, *IEEE Standard for Synchrophasor Data Transfer for Power Systems*, vol. 2011, no. December. 2011.

[6] A. Derviskadic, P. Romano, M. Pignati, M. Paolone, "Architecture and Experimental Validation of a Low-Latency Phasor Data Concentrator," in *IEEE Transactions on Smart Grid* , vol.-, no.-, pp.-.

[7] Marco Pignati, Resilient synchrophasor networks for the real-time monitoring, protection and control of power grids: from theory to validation. PhD thesis, EPFL, 2017.

[8] P. System, R. Committee, I. Power, and E. Society, *IEEE Guide for Phasor Data Concentrator Requirements for Power System Protection , Control , and Monitoring IEEE Power and Energy Society*, no. May. 2013.

[9] “IEEE Standard for Synchrophasor Measurements for Power Systems,” IEEE Std C37.118.1-2011 (Revision of IEEE Std C37.118-2005), pp. 1–61, 2011.

[10] M. Pignati, L. Zanni, P. Romano, R. Cherkaoui and M. Paolone. Fault Detection and Faulted Line Identification in Active Distribution Networks Using Synchrophasors-based Real-Time State Estimation, in IEEE Transactions on Power Delivery Pwrd, vol. 32, num. 1, p. 381-392, 2017.